THE UNIVERSITY OF CALGARY

Optimal design of Autocorrelation Functions

by

Sean M. Dougherty

A THESIS

SUBMITTED TO THE FACULTY OF GRADUATE STUDIES

IN PARTIAL FULFILLMENT OF THE REQUIREMENTS FOR THE

DEGREE OF MASTER OF SCIENCE

DEPARTMENT OF GEOLOGY AND GEOPHYSICS

CALGARY, ALBERTA

JUNE, 1986

ISBN 0-315-32646-8

THE UNIVERSITY OF CALGARY

FACULTY OF GRADUATE STUDIES

The undersigned certify that they have read, and recommend to the Faculty of Graduate Studies for acceptance, a thesis entitled, "Optimal Design of Autocorrelation Function", submitted by Sean Melbourne Dougherty in partial fulfillment of the requirements for the degree of Master of Science.

James H. Justice

Dr. J.H. Justice, Supervisor
Dept. of Geology & Geophysics

R. J. Brown

Dr. R.J. Brown
Dept. of Geology & Geophysics

E S Krebes

Dr. E.S. Krebes
Dept. of Geology & Geophysics

Jon Rokne

Dr. J.G. Rokne
Dept. of Computer Science

July 11, 1986

ABSTRACT

To improve the quality of Vibroseis data one can decrease either the width of the main peak or the energy of the sidelobes of the autocorrelation function of the vibrator sweep signal. Sweep parameters and weights can be determined so that the weighted sum of resultant autocorrelation functions exhibits minimal sidelobe energy, without significant loss of resolution.

The problem of finding an optimal linear combination of autocorrelations of realizable vibroseis sweeps is formulated as a multidimensional constrained optimization problem. A combinatorial search method is combined with a generalized inversion to obtain an approximation to the optimal solution.

Synthetic and real data examples show that for linear sweep signals the sidelobe energy of an autocorrelation function can be reduced by linear combination with other autocorrelation functions. However, the reduction in the sidelobe energy may not be significant enough to improve the visual quality of field data.

ACKNOWLEDGEMENTS

I am especially grateful to Dr. Jim Justice for his enthusiastic supervision of this project. The considerable time that was spent discussing various ideas and techniques will not be forgotten.

Many thanks to Mike Withers and Dick Miller of Group 4 Systems Ltd. for the unlimited computer time, the impromptu lessons in structured programming that they often gave, and the patience they demonstrated when I was using large portions of processing time.

Special thanks to Alberta Energy Company, in particular Keith Young, for providing moral support to the project, and for suggesting, and financially supporting, the field work. Glen Tite of Sonics Exploration Ltd. extended my knowledge of the Vibroseis technique and provided stimulating discussion of many ideas.

Paul Wellings of Academic Computer Services suggested the use of the CDC 205 Supercomputer, that allowed the range of the project to expand enormously. My thanks to Scott Cheadle who, having served a frustrating apprenticeship, taught me how to ´drive the 205´!

For help in preparation of the thesis, I would like to thank Dr. Jim Brown for a detailed critique of the text and Miriam Boody for typing the equations.

Finally, I would like to acknowledge the moral support of Ms. Lin Heidt, and my parents for encouraging enquiry long before I knew its importance.

TABLE OF CONTENTS

page

LIST OF FIGURES

page

CHAPTER I INTRODUCTION

There is an increasing demand in seismic exploration for improved data quality. To a large degree, any improvement in data quality, in terms of resolution and signal-to-noise ratio, provides a reduction in the ambiguity of the subsequent geological interpretation. In recent years, the use of high speed computers and software developments have achieved gains in seismic data processing and interpretation. However, in many areas these developments demand high quality field data and as a result, acquisition methods have placed constraints on the amount of information that can be extracted from the data.

In the Vibroseis method of seismic exploration the input signal to the earth is controlled to some extent by the user. This gives the method the advantage of flexibility in that the signal can be altered until a particular data resolution and signal-to-noise ratio is achieved, subject to constraints on the bandwidth and constraints imposed by the vibrator units, the earth, and the recording system. This thesis examines the area of signal design to find vibrator signals that, subject to the constraints on bandwidth and realizability, have both high resolution and high signal-to-noise ratio.

1.1 The Vibroseis Seismogram Trace

In seismic prospecting, a signal is introduced into the earth from on, or near, the surface. The signal, which is reflected from interfaces within the earth, is recorded at the surface. Using the convolution model of the seismic trace [61], the signal recorded at the geophones may be modelled by

$$g(t) = \{ s(t) * e(t) * r(t) \} + n(t) \qquad 1.1$$

where r(t) is the earth impulse response, n(t) is noise, s(t) is the seismic source signal, and e(t) represents the filtering effects of earth attenuation, source-earth coupling and the recording system [11]. This means that g(t) appears as a sum of progressively altered and delayed replicas of the input signal s(t) at the observed reflection times plus additive noise.

The long duration of a vibrator input signal relative to the travel time of the pressure wavefront produces returning reflection trains from various depths that overlap one another in time, making the identification of individual reflections very difficult. In addition, these reflecticn records usually have low signal-tc-noise ratios due to low instantaneous power output of the vibrator signal.

Consequently, an additional processing step, correlation, is required of the recorded data to transform these long duration field signals into an impulse-like signal. The crosscorrelation of the geophone recorded signal with the vibrator input signal compresses the extended wave trains and also improves the signal-to-noise ratio [42].

The correlation of the geophone output, g(t), and the vibrator input signal, s(t), yields the vibroseis seismogram trace

$$v(t) = s(t) \otimes g(t) \qquad 1.2$$

where $\otimes$ represents correlation. This can be shown (see Appendix A) to be equivalent to

$$v(t) = \phi_{ss}(t) * e(t) * r(t) + N(t) \qquad 1.3$$

where $\phi_{ss}(t)$ is known as the autocorrelation function of the signal s(t) defined as

$$\phi_{ss}(t) = s(-t) * s(t) \qquad 1.4$$

and N(t) is a noise component.

1.2 Autocorrelation Function Shape

An autocorrelation function is symmetrically shaped about its main peak, as seen in Fig. 1, and consists of three main components. Referring to Fig. 1, the portion of the autocorrelation from the centre peak (at the origin) to the first zero crossings is known as the main peak. The rest of the function is referred to as sidelobes with the sidelobe between the first zero crossing and the first local maximum beyond the first zero crossing known as the primary lobe [14,37].

The main peak represents the signal on the Vibroseis seismogram, and the main peak width a measure of the resolution of the signal. Since the sidelobes are the result of the correlation process, they are referred to as correlation noise [18].

1.3 Aims of the Thesis

The quality of Vibroseis data, assuming the trace model of eqn. 1.3, is determined by the shape of the function $\phi_{ss}(t)$, the effect of $e(t)$ on the shape of $\phi_{ss}(t)$, and the magnitude of $N(t)$. In this thesis, the problem of controlling the shape of the autocorrelation function $\phi_{ss}(t)$ of a signal $s(t)$ is examined.

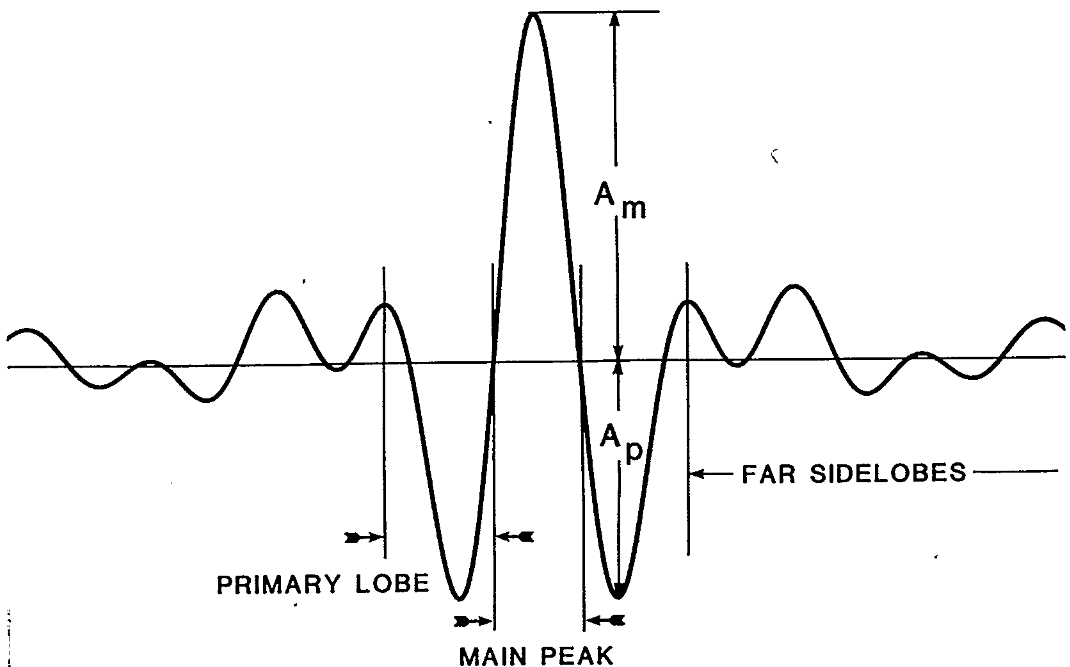

FIGURE 1 FEATURES OF AN AUTOCORRELATION FUNCTION

For high resolution and high signal-to-noise ratio, an autocorrelation must have a narrow main peak (resolution) and low sidelobe energy (correlation ncise). Ideally, the autocorrelation would be a delta function, with an infinitesimally small main peak width and zero sidelobe energy. However, a delta functicn is an infinite bandwidth signal and is unrealizable due to the finite bandwidth limitations of vibrator units and recording systems.

Obviously, the next best option is to find the autocorrelation function of signals that can be generated by a standard vibrator unit and control electronics and which has the narrowest main peak width and lowest sidelcbe energy. Unfortunately, it is not possible to minimize both these features simultaneously (see chapter II). The problem of reducing the sidelobe energy of autocorrelation functions to improve data quality in Vibroseis exploration has been considered by several authors [6,14,17,18,19,35,70] (see chapter III). However, two points that have not been previously considered are:

1. Preservation of signal resolution (main peak width) when reducing sidelobe energy, and

2. Optimal selection of signal parameters for minimizing sidelobe energy.

The aim of this thesis is to find a method of minimizing the sidelobe energy of an autocorrelation function of a signal which can be realized by a standard vibrator unit and electronics such that main peak width is not significantly increased.

CHAPTER II SIGNAL PARAMETERS & THE AUTOCORRELATION FUNCTION

2.1 Introduction

The shape of the autocorrelation function $\phi_{ss}(t)$ of a signal s(t) is determined by the parameters of s(t). In this chapter the sweep signal, as used in Vibroseis, and the effects of the parameters of the sweep signal on the shape of the autocorrelation function are described.

2.2 The Sweep Signal

In its most narrow definition, a sweep is a continuously oscillating signal with constant amplitude whose instantaneous frequency varies with time. The mathematical representation of the sweep given by Goupillaud [30] is

$$\begin{aligned} s(t) &= A \,\mathrm{Im}\,\{ \exp [\, i2\pi \int_0^t f(\tau)\, d\tau \,] \} \qquad 2.1 \\ &= A \,\mathrm{Im}\,\{ \exp [\, i2\pi\, \theta(t) \,] \} \\ &= A \sin 2\pi\, \theta(t) \end{aligned}$$

where f(t) is the instantaneous frequency at time t, and its integral, θ (t), is the sweep phase [8]. The frequency limits of the sweep are the extreme values of instantaneous frequency $f(0)$ and $f(T)$, where T is the sweep duration.

A linear sweep is a sweep whose instantaneous frequency is a linear monotonic function of time. Accordingly, sweeps whose instantaneous frequency does not vary linearly with time are called nonlinear sweeps (Fig. 2). Nonlinear sweeps are not necessarily monotonic. In this thesis, only linear sweeps will be considered because:

1. For a particular start and end frequency there is only one linear sweep, whereas there are an infinite number of possible nonlinear sweeps. Thus, by considering only linear sweeps the number of degrees of freedom in the problem is reduced, making the problem manageable.

2. Vibrator units can generate linear sweeps within a finite bandwidth range but cannot necessarily generate a specific nonlinear sweep.

For a linear sweep, with frequencies $f(0)$ and $f(T)$ at time $t = 0$ and time $t = T$ respectively, the instantaneous frequency can be defined by

$$f(t) = f(0) + (f(T) - f(0))(t/T) \qquad 2.2$$

for which the phase is given by

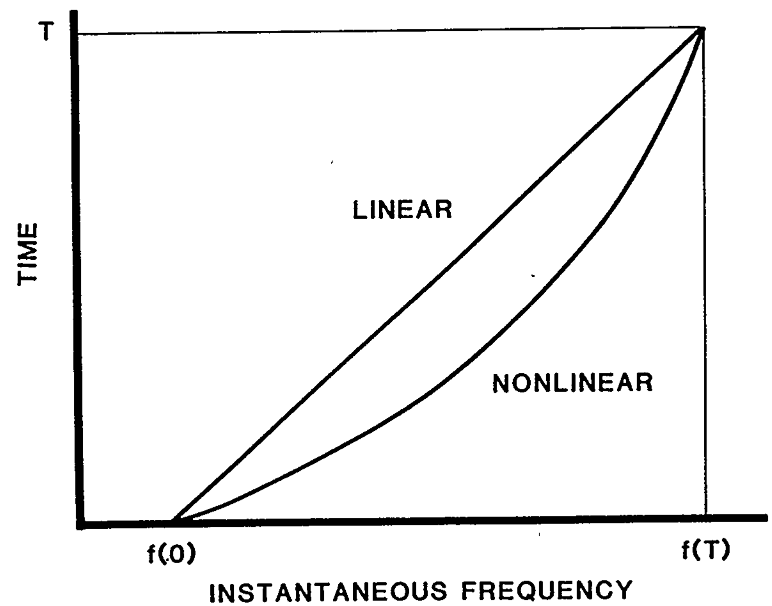

FIGURE 2 INSTANTANEOUS FREQUENCY AS A FUNCTION OF TIME FOR LINEAR & NONLINEAR SWEEPS

$$\theta(t) = f(0)t + (f(T) - f(0))(t^2/2T). \qquad 2.3$$

In addition, let the frequency limits be defined as

$$f_L \leqq f(0) \leqq f(T) \leqq f_H. \qquad 2.4$$

The linear sweep signal defined by eqn. 2.1, with phase defined by eqn. 2.3, is a function of start frequency f(0), end frequency f(T), and duration T. The autocorrelation function of the sweep signal, as defined by eqn. 1.4, is a function of the same parameters (see [35,39,59] for analytic expressions for the autocorrelation function of a linear sweep with phase defined in eqn. 2.3).

2.3 Shape of the Autocorrelation Function of Linear Sweeps

The shape of an autocorrelation function of a signal is determined by the parameters of the signal. As seen in section 2.2, a linear sweep signal is a function of the start and end frequency, f(0) and f(T), of the sweep and the sweep duration T.

The start and end frequency of a linear sweep determine both the width of the main peak and the amplitude of the sidelobes. Firstly, define the centre frequency of a linear sweep signal as

$$f_c \equiv \frac{1}{T_c} = \frac{1}{2}\left(f(0) + f(T) \right) \qquad 2.5$$

where T_c is the period of the centre frequency, and the ratio of the end frequencies of the sweep as

$$R_f = \frac{f(0)}{f(T)} \qquad 2.6$$

The width of the main peak, defined as the absolute value of the time interval between the first positive and negative zero crossings on either side of the main peak, as shown in Fig. 1, is given by T_c / 2 [28]. For this definition of width it can be easily seen that the width of the main peak is determined by the sum of the end frequencies of the sweep;

<u>ie</u>. $$\frac{T_c}{2} = \frac{1}{2f_c} = \frac{1}{f(0) + f(T)} \qquad 2.7$$

Thus, the larger the sum of the end frequencies of the sweep, the smaller the width of the main peak (Fig. 3).

The amplitude of the largest sidelobe <u>i.e</u>. the primary lobe, relative to the main peak amplitude, is dependent on R_f, the ratio of the end frequencies of the sweep [28]. Decreasing R_f reduces the primary sidelobe-main peak

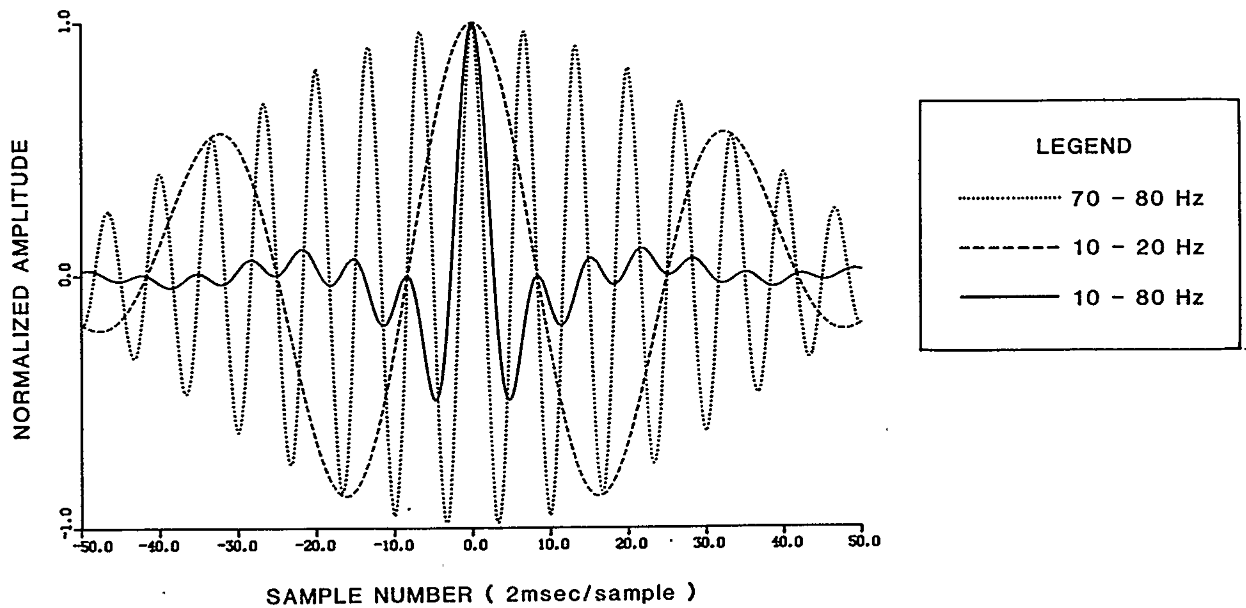

FIGURE 3 EFFECT OF DIFFERENT START & END FREQUENCIES ON THE AUTOCORRELATION FUNCTIONS OF LINEAR SWEEPS IN THE FREQUENCY BAND 10 - 80 Hz

amplitude ratio (Fig. 3).

As can be seen in Fig. 3, it is not possible to minimize both main peak width and sidelobe energy simultaneously. Consider the example where the frequency of the linear sweep is constrained as in eqn. 2.4. Main peak width is minimized when the sum of the end frequencies is maximized (eqn. 2.7). This occurs when $f(0) = f(T) = f_H$. The primary lobe-main peak amplitude ratio is minimized (eqn. 2.6) when the ratio $f(0)/f(T)$ is minimized which occurs when $f(0) = f_L$ and $f(T) = f_H$ i.e. occurs for the linear sweep with the largest bandwidth. Obviously, the two features are minimized for different linear sweeps within the same bandwidth.

The sweep duration determines the duration of the autocorrelation function. A sweep s(t) defined for $0 \leqq t \leqq T$ has an autocorrelation defined for $-T \leqq t \leqq T$ [20]. Also, increasing the duration of the sweep increases the total energy of the autocorrelation [35].

2.4 Summary

Summarizing the major points:

1. A linear sweep signal is a function of start frequency

f(0), end frequency f(T) and sweep duration T.

2. The sum of the start and end frequencies of a linear sweep determines the width of the main peak of the autocorrelation function and the ratio of the start and end frequencies determines the primary sidelobe-main peak amplitude ratio.

3. Both main peak width and primary lobe-main peak amplitude ratio cannot be minimized simultaneously.

4. Sweep duration determines the duration and the total energy of the autocorrelation function.

It can be seen that the start and end frequencies of a linear sweep signal have a more significant effect on the shape of the autocorrelation function of the sweep than the sweep duration. Thus, unless otherwise stated, it will be assumed that sweep duration T is a constant.

CHAPTER III PROBLEM FORMULATION

3.1 Previous Work

The aim of the thesis, described in section 1.3, is to find a method of minimizing the sidelobe energy of an autocorrelation function of a signal that can be generated by a standard vibrator and control electronics such that main peak width remains constant. The problem has been further constrained by only allowing linear sweeps between the frequencies f_L and f_H where $f_L \leq f_H$ (see section 2.2).

An easily implemented, simple method of reducing sidelobe energy is tapering the amplitude of the sweep signal at each end [17,35]. However, amplitude tapering increases main peak width [5] i.e. tapering reduces resolution, which is an undesirable effect. A method of linearly combining individual autocorrelation functions, called Combisweep, was shown to reduce primary lobe amplitude and far sidelobe energy of autocorrelations [19,70]. However, these observations were noted for arbitrarily chosen linear sweep signals, the sweep parameter selection not being optimal in any sense.

In radar research there has been considerable interest in optimal autocorrelation function synthesis [16,20,63,69].

Many of the treatments of the problem worked directly with the autocorrelation function shape of a signal, subject to constraints on the spectrum of the function, and then found the signal by factorization [16,63]. Using this approach constraints on the signals were not applied and the solution signals were unrealizable. A more successful method considered the signals directly, with constraints on sidelobe energy and bandwidth [20]. The method aimed to find signals s from the set of all real numbers $\mathbb{R}$, that minimized

$$|| \phi_{ss} - \phi_D || \qquad 3.1$$

where ϕ_D is an autocorrelation with a desired shape. $||\cdot||$ denotes the norm.

The optimal approach of Evans et al. [20] and the combination of autocorrelations suggested by Werner and Krey [70] suggest a method to solve the thesis problem.

3.2 Formulation of a Method

If a linear sweep signal s is a function of start frequency f(0), end frequency f(T) and time t (see chapter II), then the autocorrelation function of s, as defined by eqn. 1.4, is a function of the same variables. Consider a weighted linear combination of N normalized autocorrelations:

$$\sum_{K=1}^{N} a_K \, \phi_{ss,K} \left(f_K(0),\ f_K(T),\ t \right) \quad a_K \in \mathbb{R} \qquad 3.2$$

where a_j is the weighting factor applied to the jth autocorrelation function ϕ_j , itself a function of $f_j(0)$ and $f_j(T)$, and $\mathbb{R}$ is the set of all real numbers. The functions are normalized such that the main peak amplitude $A_m = 1$. This is essentially a formulation of the autocorrelation combination considered by Werner and Krey, where they assumed that $a_K = 1$ for all k. Allowing $a_K \in \mathbb{R}$ is a simple generalization of the autocorrelation combination that they considered.

Let a normalized autocorrelation that has a desired shape, e.g. narrow main peak and zero sidelobe energy, be ϕ_D. Then, similarly to eqn 3.1, the thesis problem can be posed: to find $s_K \in V$ and $a_K \in \mathbb{R}$ that minimize

$$\left|\left| \sum_{K=1}^{N} a_K \, \phi_{ss,K} \left(f_K(0),\ f_K(T),\ t \right) - \phi_D \right|\right| \qquad 3.3$$

where V is the set of signals defined by

$$s(t) = A \sin 2\pi \left\{ f(0)t + \left(f(T) - f(0) \right) \frac{t^2}{2T} \right\} \qquad 3.4$$

and $f_L \leqq f(0) \leqq f(T) \leqq f_H$.

This formulation of the thesis problem is not a unique method for achieving the aims of the thesis but it has the important feature of being based on the combination of two techniques that, individually, have been demonstrated to improve autocorrelation function shape.

3.3 Application of the Method

The application of eqn. 3.3 to achieving the aims of the thesis is dependent of the choice of ϕ_D and the autocorrelation function for which the sidelobe energy is to be reduced. As shown in section 2.3, within the frequency constraint of eqn. 2.4, the autocorrelation function that has the lowest sidelobe energy is generated by the linear sweep with the largest bandwidth ($f_H - f_L$). It seems reasonable to select this autocorrelation function as the autocorrelation for which the sidelobe energy is to be minimized. Let this autocorrelation be ϕ_A, and then let $\phi_1 = \phi_A$.

To reduce the sidelobe energy of ϕ_A by minimizing the norm of the difference between a linear combination of ϕ_A and other autocorrelations, ϕ_D must have the same main peak as ϕ_A and zero sidelobe energy. By selecting such a ϕ_D the method should not alter the main peak shape of ϕ_A and thus the main peak width is preserved whilst sidelobe energy is reduced. If ϕ_D did not have the same main peak as ϕ_A then the method would attempt to change both the main peak and the sidelobe energy of ϕ_A to that of ϕ_D. In doing this, the change in sidelobe energy may not be as significant as when the method is attempting to only minimize sidelobe energy. (The dependence of the method on the choice of ϕ_D is discussed in chapter V).

Summarizing, the autocorrelation whose sidelobe energy is to be reduced is the autocorrelation function of the linear sweep with the largest bandwidth ϕ_A. Thus $f_1(0) = f_L$ and $f_1(T) = f_H$. To reduce the sidelobe energy of ϕ_A, ϕ_D is chosen with zero sidelobe energy and the same main peak as ϕ_A.

CHAPTER IV PROBLEM SOLUTION

4.1 Introduction

The thesis problem has been formulated as a multidimensional constrained optimization problem to find sweeps $s_K \varepsilon V$ and $a_K \varepsilon \mathbb{R}$ such that

$$|| \sum_{K=1}^{N} a_K \phi_{ss,K} (f_K(0), f_K(T), t) - \phi_D || \qquad 4.1$$

is minimized. As discussed in section 3.3, $f_1(0) = f_L$ and $f_1(T) = f_H$ since $\phi_1 = \phi_A$. Thus solving eqn 4.1 requires N - 1 values for both $f_k(0)$ and $f_k(T)$ and N values for a_k.

In practice, geophysical data is discretely sampled and it is appropriate to consider the problem in a discrete form. For a sweep s_j, M samples in length, the ith sample of its autocorrelation ϕ_i is given by

$$\phi_i = \sum_{j=1}^{M} s_{j+i} s_j \qquad 4.2$$

where the length of the autocorrelation function is 2M - 1 samples with the main peak at i = 0. The pth norm for a function g_i, L samples in length, can be defined by

$$[\sum_{i=1}^{L} g_i^p]^{1/p} \qquad 4.3$$

and thus eqn 4.1 can be rewritten

$$\left[\sum_{i=-M}^{M} \left(\left\{ \sum_{K=1}^{N} a_K \left(\sum_{j=1}^{M} s_{j+i} s_j \right)_K \right\} - \phi_{D,i} \right)^p \right]^{1/p} \qquad 4.4$$

where $\phi_{D,i}$ is the ith sample of ϕ_D, and $\left(\sum_{j=1}^{M} s_{j+1} s_j \right)_K$ is the ith sample of the kth autocorrelation function i.e. $\phi_{K,i}$, which is a function of $f_k(0)$ and $f_k(T)$.

The problem is now to minimize the function expressed by eqn. 4.4. This represents a discrete (3N - 2)-dimensional constrained optimization problem, with constraints on the allowable signal set ($s_K \varepsilon V$) and the weights ($a_K \varepsilon \mathbb{R}$). The minimum of eqn. 4.4 could be found using a variety of methods [50]. Gradient methods, in particular gradient search methods [22,23,55], are commonly used but difficulties can arise with local minima and the initial 'guess' of solutions.

A method that guarantees finding the discrete global minimum of eqn. 4.4, within the constraints, is to calculate the norm values for all possible combinations of the sweep parameters. Let this approach be called a combinatorial search method.

4.2 Solution of $f_k(0)$ and $f_k(T)$ by Combinatorial Search

The combinatorial search method used to solve for $f_k(0)$ and $f_k(T)$ ($k = 2,..,N$) examines all possible combinations of f(0) and f(T) allowed by the frequency constraint defined in eqn. 2.4. The major advantage of a combinatorial search method for solving for $f_k(0)$ and $f_k(T)$ is that the discrete global minimum within the constraints on the parameters is always located i.e. the method is stable. Also, the method is ideally suited for computer implementation. Unfortunately, the amount of computation time involved in a combinatorial search is very high. It is therefore important to reduce the number of calculations required.

The total number of combinations of the frequency parameters that have to be examined determines the computation time to reach a solution to eqn. 4.1. The number of combinations involved is determined by the size of f_L and f_H and how closely the frequencies are sampled, and upon how the combinatorial method is applied to solve eqn. 4.1.

The combinatorial method can be applied to solving eqn. 4.1 in two different ways, with a major difference in the number of parameter combinations that have to be considered. Assume that the frequency constraints allow P different combinations of f(0) and f(T) *i.e.* P frequency parameter pairs. If the problem is considered for one additional autocorrelation function at a time *i.e.* if one solves for $f_2(0)$ and $f_2(T)$ in

$$a_1\phi_A + a_2\phi_2 \,(\, f_2(0),\ f_2(T)\,)$$

and then, having solved for $f_2(0)$ and $f_2(T)$, one solves for $f_3(0)$ and $f_3(T)$ in

$$a_1\phi_A + a_2\phi_2 + a_3\phi_3 \,(\, f_3(0),\ f_3(T)\,)$$

up to N-1 autocorrelations combined with ϕ_A, then

$$P(\,N - 1\,) - N\,(\,N - 1\,)/2 \qquad 4.5$$

frequency parameter pairs have to be considered (see Appendix B). If N-1 additional autocorrelations are considered together *i.e.* if one solves for $f_2(0),\ldots,f_N(0)$ and $f_2(T),\ldots,f_N(T)$ in

$$a_1\phi_A + a_2\phi_2\,(\, f_2(0),\ f_2(T)\,) + \ldots + a_N\phi_N\,(\, f_N(0),\ f_N(T)\,),$$

then the number of frequency parameter pairs that are considered (see Appendix B) is

$$(P - 1)! / (P - N)!(N - 1)! \qquad 4.6$$

For P >> N the number of parameter pairs considered for the two methods is approximately P(N-1) and $P^{(N-1)}/(N-1)!$ respectively. Obviously, the relative number of parameter pairs to be considered by each method is dependent on the size of P and N.

The magnitude of P is determined by f_L and f_H and the frequency interval used to sample the frequencies. For this project the frequencies were sampled at 1 Hz intervals as it was felt that the difference in autocorrelation shape for a change in bandwidth of less than 1 Hz was negligible, but for a change greater than 1 Hz, it may not be negligible. Then, for example, if f_L = 10 Hz and f_H = 100 Hz, the total number of combinations of frequency parameters satisfying eqn. 2.4 is 4186.

For P = 4186 and, for example, N = 3, the method of considering all autocorrelation functions simultaneously requires approximately 1050 times more frequency parameter combinations to be considered. Even for small N the difference between the number of frequency parameter pairs that are examined in each method is considerable. The much larger number of parameter pairs that have to be considered when all N autocorrelation functions are considered simultaneously dictated that this method of applying the combinatorial search was not used even though it may provide a more optimal solution to eqn. 4.1 than the method of considering one additional autocorrelation function at a time.

4.3 Solving For Weighting Factors

The thesis problem of eqn 4.1 can be written in matrix form: to find the vector **a** = (a_1, a_2,.., a_N) that solves

$$\min \; || \; \Phi \, a - \Phi_D \; ||_p \qquad 4.7$$

where, for autocorrelation functions (2M-1) samples in length, and using the method of solving for only one additional autocorrelation at a time, Φ is a (2M-1) x k matrix defined by

$$\Phi = \begin{bmatrix} \phi_A(-M) & \phi_2(-M) & \cdots & \phi_K{}^{(R)}(-M) \\ \phi_A(0) & \phi_2(0) & \cdots & \phi_K{}^{(R)}(0) \\ \phi_A(M) & \phi_2(M) & \cdots & \phi_K{}^{(R)}(M) \end{bmatrix} \qquad 4.8$$

where: ϕ_A, ϕ_2, ..., ϕ_{K-1} are fixed, and $\phi_K{}^{(R)}$ is the kth autocorrelation in the linear combination of N autocorrelation functions for which $f_k{}^{(R)}(0)$ and $f_k{}^{(R)}(T)$

are the Rth frequency parameter pair to be selected combinatorially, $1 \leqq R \leqq P - k + 1$ (see Appendix B), and Φ_D is a (2M-1) dimensional vector defined by

$$\Phi_D = (\phi_D(-M), \phi_D(-M+1), \ldots, \phi_D(0), \ldots, \phi_D(M)) \qquad 4.9$$

If the norm in eqn 4.7 is the case $p = 2$, or the L_2 norm, then there is a unique solution to eqn 4.7 given by the vector

$$a' = (a_1, a_2, \ldots, a_R) = \Phi^I \Phi_D \qquad 4.10$$

where Φ^I is the generalized inverse of Φ [41,54].

It can be shown [54] that the generalized inverse Φ^I of a matrix Φ is given by

$$\Phi^I = (\Phi^* \Phi)^I \Phi^* \qquad 4.11$$

or

$$= \Phi^* (\Phi \Phi^*)^I \qquad 4.12$$

where Φ^* is the transpose of Φ. When calculating Φ^I, a choice is made between eqn. 4.11 and eqn 4.12 according to whether $\Phi^*\Phi$ or $\Phi\Phi^*$ has smaller order. As shown in eqn. 4.8, Φ is a (2M-1) X k matrix. M is of the order of 1000 and $k \leqq 20$ (see chapter 5) and thus eqn. 4.11 was used to calculate

Φ^I. Details of how to calculate $(\Phi^*\Phi)^I$ can be found in [31].

4.4 Description of the Solution Algorithm

Now that all the different parts of the solution method have been discussed, a step-by-step description of the algorithm for finding autocorrelation functions that minimize the sidelobe energy of the autocorrelation function of the largest bandwidth linear sweep can be given.

1. A normalized autocorrelation function ϕ_D with a desired shape is chosen.

2. k = 1. The frequency parameters $f_1(0)$ and $f_1(T)$ are known and give the autocorrelation function ϕ_A, which is normalized. For this case the solution for a_1 is trivial, with $a_1 = 1$.

3. k = 2 and R = 1. Select a frequency parameter pair, $f_2{}^{(1)}(0)$ and $f_2{}^{(1)}(T)$, and calculate the corresponding normalized autocorrelation function $\phi_2{}^{(1)}$.

4. Calculate Φ using the definition of eqn. 4.8, and its generalized inverse Φ^I, and solve for a_1 and a_2 for $\phi_2{}^{(1)}$.

5. Calculate the L_2 norm of

$$a_1\phi_A + a_2\phi_2 \;(\; f_2^{(1)}(0),\; f_2^{(1)}(T)\;) - \phi_D$$

6. Repeat steps 3 to 5 for R = 2 up to R = P - k + 1 i.e. for each frequency parameter pair that satisfies the frequency constraint given by eqn. 2.4.

7. When the L_2 norm values for all possible ϕ_2, generated from all possible different frequency parameter pairs, have been calculated, find the minimum L_2 norm value. The frequency parameter pair and the weighting factors that correspond to the minimum L_2 norm value are selected as the optimal parameter pair and optimal weights for ϕ_2.

8. Steps 3 to 7 are repeated for k = 3, up to k = N. When the optimal $f_N(0)$ and $f_N(T)$ have been found, then a solution for the linear combination of N autocorrelation functions has been reached.

4.5 Extending the Solution Method

The combinatorial method of solving for the start frequency and end frequency variables can easily be extended to solve for more variables or to allow different constraints on the sweep signal set. The sweep signal as defined in section 2.2 is at most a function of three variables: start frequency f(0), end frequency f(T) and duration T. Amplitude is not considered as it is incorporated in the weighting factors. If, for example, it is desirable to solve for all three variables using the combinatorial search method, the only change to the two-variable case is an increase in the number of parameter combinations that have to be considered. If there are P frequency parameter pairs and Q different values of signal duration, then the total number of combinations of f(0), f(T), and T is PQ. Thus, for the method where only one additional autocorrelation function is considered at a time then the total number of parameter combinations that have to be examined is approximately PQ(N - 1).

One major advantage of the solution method described is that it is independent of the constraint ranges of the parameters or the definition of the input sweep signal. Allowing the constraint range of the variables to increase or decrease can be achieved with, respectively, only an increase or decrease in the number of parameter combinations considered. Since the method of solution is independent of the input signal definition, other sweep definitions can be considered without having to alter the solution method.

Obviously, the major restriction to increasing the size of the problem when using a combinatorial search method to find a solution is the total computation time required. However, it is seen that the method can be extended with ease to include more variables and different constraint ranges for the parameters but at the expense of computation time.

4.6 Summary

1. A combinatorial search method is used to find solutions to eqn. 4.1. The advantages of this type of solution are: a) it locates the discrete global minimum of the norm, or error, surface (eqn. 4.4) within the constraint ranges of the variables; b) it can be easily implemented by computer, and c) it can be easily extended to include more variables.

2. The number of calculations involved, and thus the computation time, to reach a solution to eqn. 4.1 is dependent on the total number of combinations of the variables under consideration. By considering only one additional autocorrelation function at a time, the number of combinations of the variables considered, and consequently calculations, is significantly reduced. The solutions given by this method may be sub-optimal but the computation size of the problem restricts the application of the combinatorial search to only considering one additional

autocorrelation at a time.

3. Solving for the weighting factors using a generalized inverse method gives a unique minimum norm value for a particular definition of Φ .

CHAPTER V RESULTS

5.1 Introduction

In this chapter, results of several experiments on the thesis method are discussed. These experiments were designed to answer several questions about the method:

1. Does the method reduce sidelobe energy ?

2. Is main peak resolution preserved ?

3. To what extent are the changes in the shape of ϕ_A dependent on the choice of ϕ_D ?

4. What is the maximum number of autocorrelation functions that need to be considered ?

5. Does the calculation of weighting factors i.e. $a_K \in \mathbb{R}$, give better results than when weights are not calculated i.e. $a_K = 1$?

6. Does the method work in the field ?

Results of both computer tests and field tests are presented.

5.2 Input Parameters and Measurements for Computer Tests

The algorithm described in section 4.4 was implemented on a CDC 205 supercomputer. The program was designed to allow input of user specified parameter values and ranges. The output included norm values calculated for each parameter combination, and the solutions to eqn. 4.1.

5.2.1 Input Parameters

For the computer tests, input parameters for the sweeps were dictated by the parameters to be used in the associated field work. All the sweeps were linear sweep signals, as defined in eqn. 3.4, of 6 seconds duration, sampled at 2 msec/sample. A 250 msec cosine taper [38] was applied to each end for practical reasons. The frequency parameters were constrained as follows:

$$8 \text{ Hz} \leqq f(0) \leqq f(T) \leqq 85 \text{ Hz}. \tag{5.1}$$

This implied that the bandwidth constraint was

$$0 \text{ Hz} \leqq f(T) - f(0) \leqq 77 \text{ Hz}. \tag{5.2}$$

ϕ_A, the first sweep in the linear combination, was an 8 - 85 Hz sweep, the sweep with the largest bandwidth within the constraints described above. The total number of autocorrelation functions considered in the experiments was set to the largest number that available computer time would allow. As a result N varied between 3 and 20.

5.2.2 Choices for ϕ_D

As discussed in section 3.3, to reduce the sidelobe energy of ϕ_A, ϕ_D was chosen with the main peak of ϕ_A and zero sidelobe energy. Let this symmetrical function be ϕ_M (Fig. 4b). To investigate how the shape of ϕ_A, in particular the sidelobe energy, is affected by the choice of ϕ_D, two other symmetrical functions were chosen.

A delta function, which has an infinitesimally small main peak width and zero sidelobe energy (Fig. 4a) was selected to examine the extent to which the method reduces both sidelobe energy and main peak width of ϕ_A. A symmetrical function with the same main peak and primary lobe as ϕ_A was selected to examine the ability of the method to reduce only far sidelobe energy. Let this function be ϕ_{MP} (Fig. 4c).

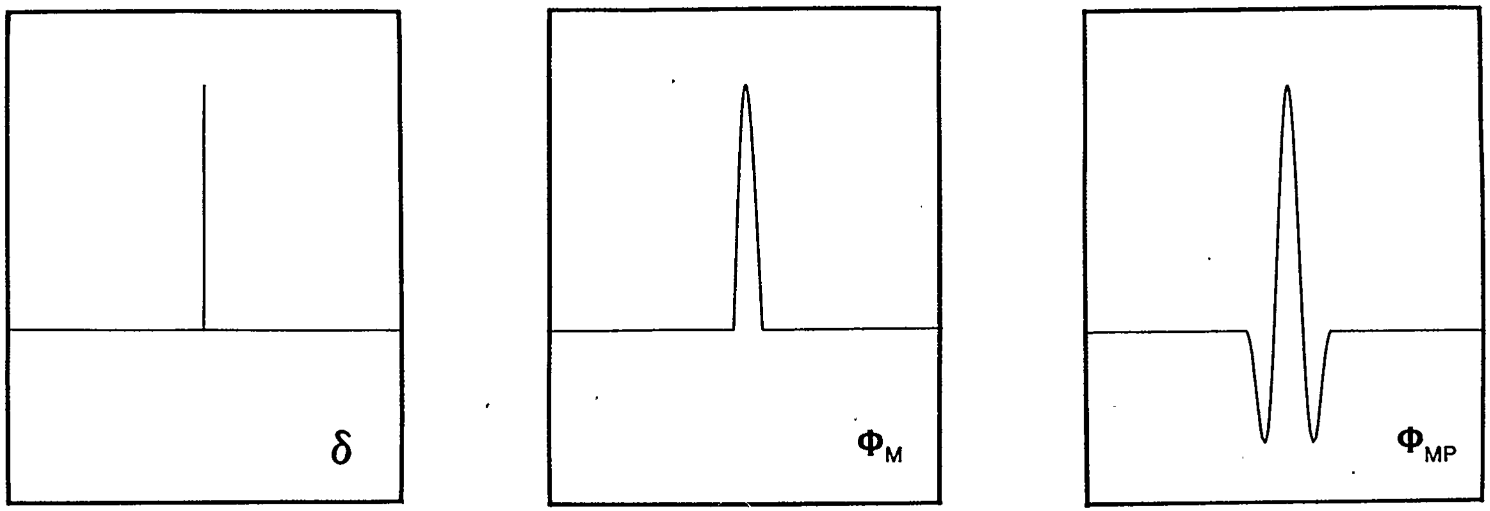

FIGURE 4a
DELTA FUNCTION

FIGURE 4b
MAIN PEAK OF Φ_A

FIGURE 4c
MAIN PEAK & PRIMARY LOBE OF Φ_A

FIGURE 4 DESIRED AUTOCORRELATION FUNCTIONS

5.2.3 Measurements

To monitor the changes in the shape of ϕ_A as a result of linear combination with other, optimally selected, autocorrelation functions, the differences in various measurements and their initial values after the addition of each successive autocorrelation function were examined. The change of a particular measurement, x, from the initial value for ϕ_A, x_A, was taken to be:

$$x_{dB} = 20 \log_{10} \left(\frac{x}{x_A} \right)$$

where x_{dB} is known as the decibel value of x relative to x_A [1]. Measurements were made of:

1. Total sidelobe energy.
2. Far sidelobe energy.
3. Primary sidelobe-Main peak amplitude ratio i.e. A_p/A_m (see Fig. 1).

To calculate the sidelobe energy E_w, the definition:

$$E_w = 2 \sum_{i=w}^{M} \left[\sum_{K=1}^{N} a_K \phi_{K,i} \right]^2 \qquad 5.3$$

where $\sum_{K=1}^{N} a_K \phi_{K,i}$ represents the ith sample of the linear combination of N autocorrelation functions, each 2M-1 samples in length, and $w = z_1$ or z_2 are the sample numbers of the first zero crossing and the first local maximum from the main peak respectively. These give the total sidelobe energy ($w = z_1$) and far sidelobe energy ($w = z_2$). It should be noted that, for normalized autocorrelation functions, $A_m = 1$ and therefore $A_p/A_m = A_p$.

The optimal frequency parameter pair and optimal weights for the kth autocorrelation function in eqn. 4.4, when solving for only one autocorrelation function at a time, yield an L_2 norm value that is the minimum L_2 norm value for the combination of k autocorrelation functions (see section 4.4). The change in the minimum norm value after the addition of each successive autocorrelation function was examined as it provides a measure of the convergence to the minimum of eqn. 4.4.

5.3 Observations and Discussion of Computer Tests

Observations from the computer tests on the method for each of the three choices of ϕ_D, namely δ, ϕ_M and ϕ_{MP}, and the effects of the different constraints on the weighting factors are described. A discussion of the observations is then given.

5.3.1 Observations for $\phi_D = \phi_M$

The minimum norm values when $\phi_D = \phi_M$ decrease for $N \leqq 3$ but then remain relatively constant up to $N = 17$, as shown in Fig. 5. The decrease in the minimum norm values corresponds to a decrease in the primary lobe amplitude for $N \leqq 4$ which, except for a small increase at $N = 5$, becomes relatively constant for all other values of N examined (Fig. 6).

The primary lobe amplitude energy, of ϕ_A is reduced by as much as 30%. This implies that the primary lobe energy is reduced. Accompanying this reduction in primary lobe energy, the far sidelobe energy (Fig. 7) of ϕ_A is increased by 10% for $N = 2$, and except for a small decrease at $N = 5$ that coincides with the small increase in primary lobe amplitude, remains relatively constant for all additional autocorrelations examined.

Total sidelobe energy of ϕ_A is reduced by only 10% for $N \leqq 5$, but then suddenly is reduced to approximately 48% for $N = 6$ (Fig. 8). This sudden decrease is explained by an increase in main peak width of 1 sample <u>i.e</u>. 2 msec, that occurs at $N = 6$. Since total sidelobe energy and primary lobe amplitude are relatively constant for $6 \leqq N \leqq 17$, it is reasonable to suggest that the main peak width only

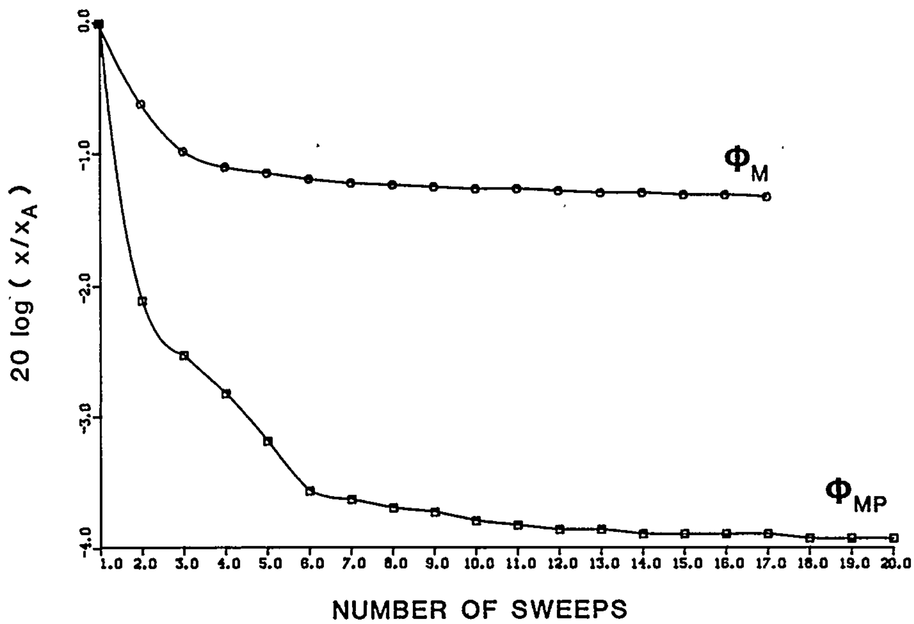

FIGURE 5 MINIMUM NORM VALUES VS. N FOR $\Phi_D = \Phi_M$ & Φ_{MP}

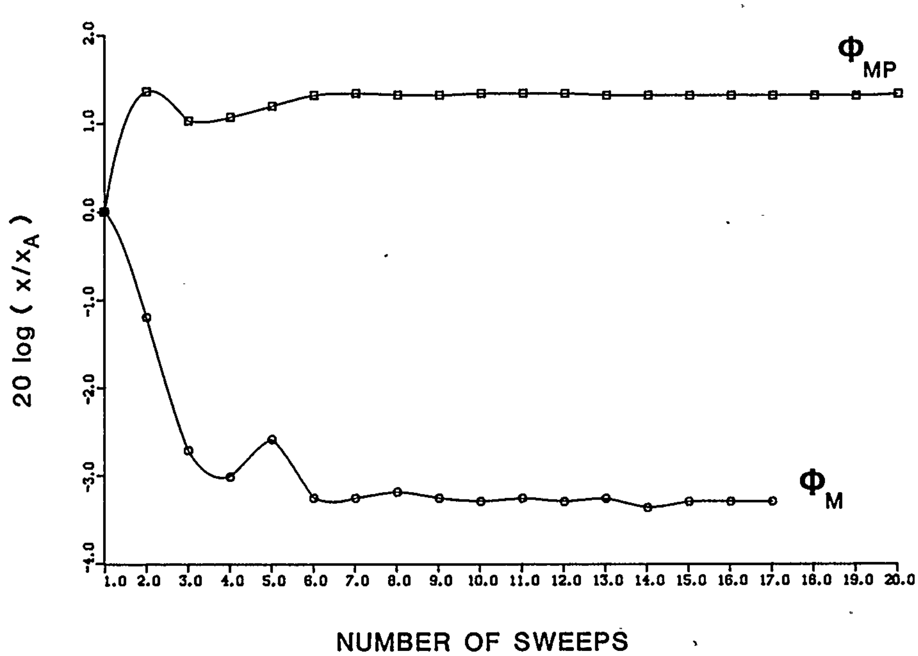

FIGURE 6 A_p / A_m VS. N FOR $\Phi_D = \Phi_M$ & Φ_{MP}

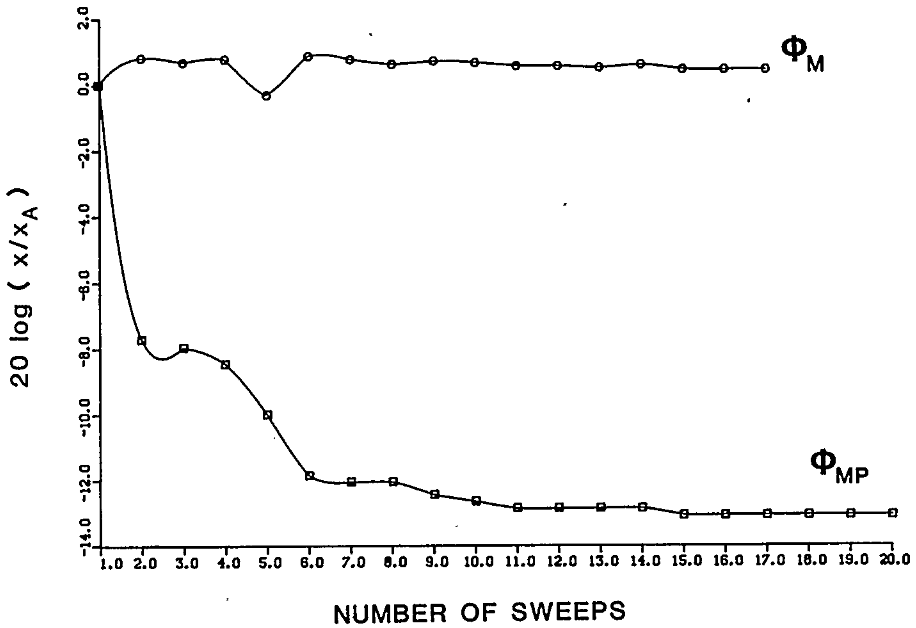

FIGURE 7 FAR SIDELOBE ENERGY VS. N FOR $\Phi_D = \Phi_M$ & Φ_{MP}

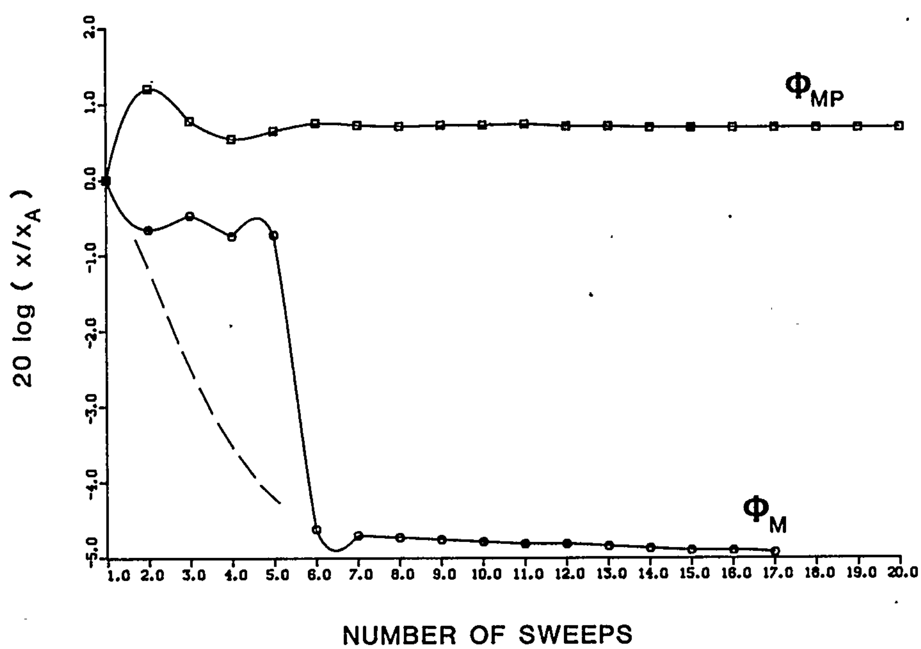

FIGURE 8 TOTAL SIDELOBE ENERGY VS. N FOR $\Phi_D = \Phi_M$ & Φ_{MP}

increases for $N \leqq 6$.

Fig. 9 shows the resultant half-autocorrelation combination for N = 3 when $\phi_D = \phi_M$. It is immediately apparent that the overall change in the shape of ϕ_A is not very significant but the reduction in the primary lobe amplitude and the small increase in the main peak width are noticeable. A change in the character of the first few sidelobes is seen, with the second zero crossing for N = 3 not occurring until the 30th sample from the centre of the main peak.

5.3.2 Observations for $\phi_D = \phi_{MP}$

When $\phi_D = \phi_{MP}$, there is a more significant decrease in the minimum norm value from its initial value for ϕ_A than occurred when $\phi_D = \phi_M$. As seen in Fig. 5, the minimum norm decreases rapidly for $N \leqq 3$, continues to drop until N = 6, and then becomes relatively constant up to N = 20. This decrease in the norm value coincides with a decrease in the far sidelobe energy (Fig. 7), which decreases rapidly for $N \leqq 3$, continues to decrease until N = 6, and then only decreases slightly up to N = 20.

Examination of Fig. 7 shows a reduction in the far sidelobe energy of ϕ_A greater then 50% for $2 \leqq N \leqq 20$ i.e.

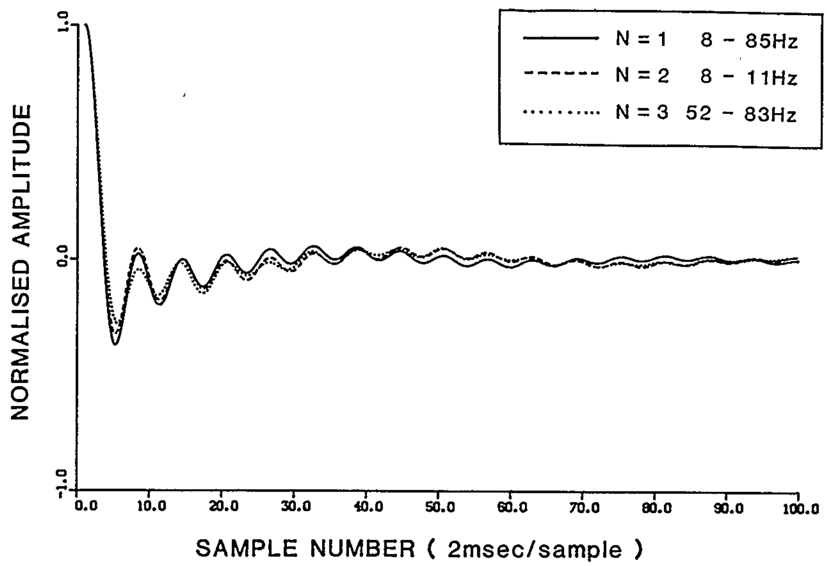

FIGURE 9 RESULTANT AUTOCORRELATION FUNCTION COMBINATIONS ($N \leq 3$) FOR $\Phi_D = \Phi_M$

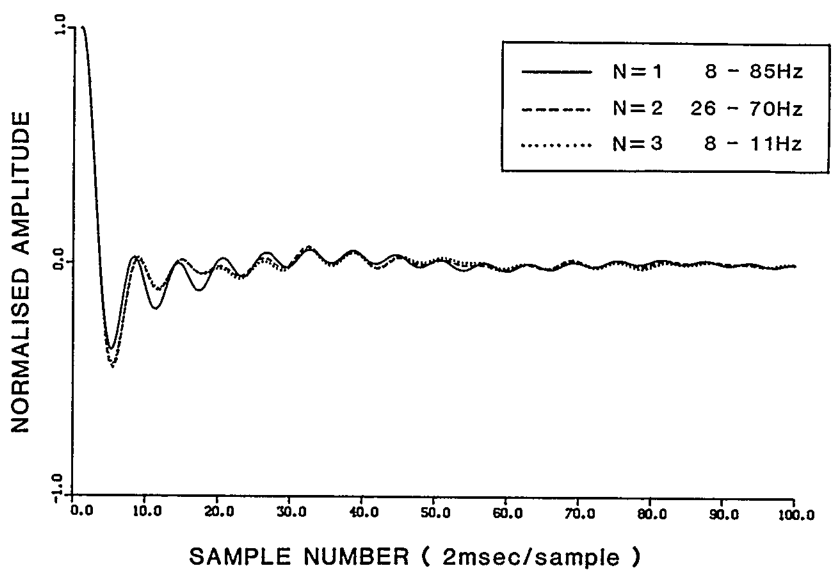

FIGURE 10 RESULTANT AUTOCORRELATION FUNCTION COMBINATIONS ($N \leq 3$) FOR $\Phi_D = \Phi_{MP}$

for all additional autocorrelation functions. The primary lobe amplitude is increased by 17% for N = 2 and, after decreasing slightly for $3 \leqq N \leqq 6$, returns to 17 % greater than the initial value for ϕ_A. However, the total sidelobe energy is increased for $2 \leqq N \leqq 20$ (Fig. 8) indicating that the increase in primary lobe energy is greater than the decrease in far sidelobe energy.

Fig. 10 shows the resultant autocorrelation combination for N = 3 when $\phi_D = \phi_{MP}$. The decrease in the far sidelobes and the increase in the primary lobe amplitude are the noticeable features of the three-autocorrelation combination. Also, it should be noticed that there is no change in the main peak width. However, the overall change in ϕ_A is again not particularly significant.

5.3.3 Observations for $\phi_D = \delta$

Fig. 11 compares observations of minimum norm values, far sidelobe energy, primary lobe amplitude and total sidelobe energy for $\phi_D = \delta$ when $N \leqq 3$ to the observations for $\phi_D = \phi_M$ and ϕ_{MP} for $N \leqq 3$. There is a small decrease in the minimum norm values (Fig. 11a) that, by examination of Figs. 11b & 11c, can be explained by a small decrease in the amplitude of the primary lobe. Since the far sidelobe energy remains almost unchanged (Fig. 11c), the total

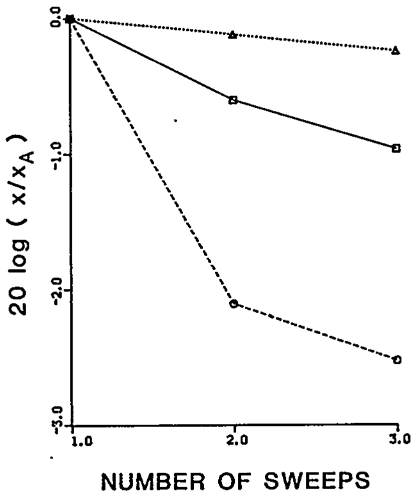

FIGURE 11a MINIMUM NORM VALUES

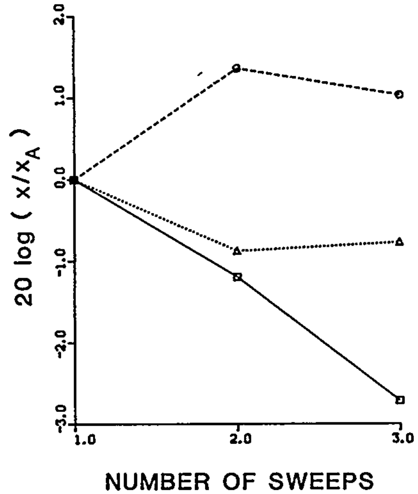

FIGURE 11b A_p / A_m

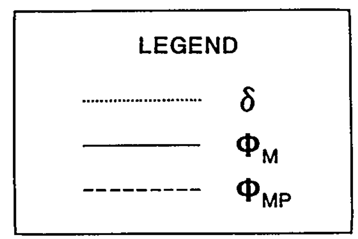

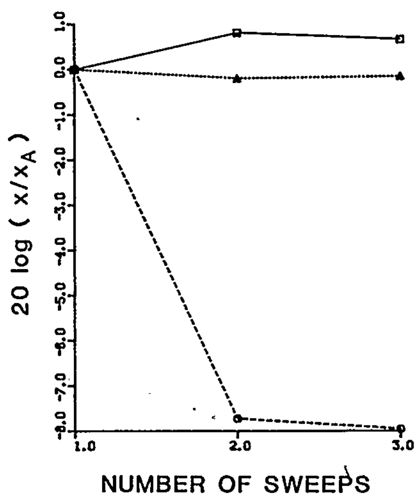

FIGURE 11c FAR SIDELOBE ENERGY

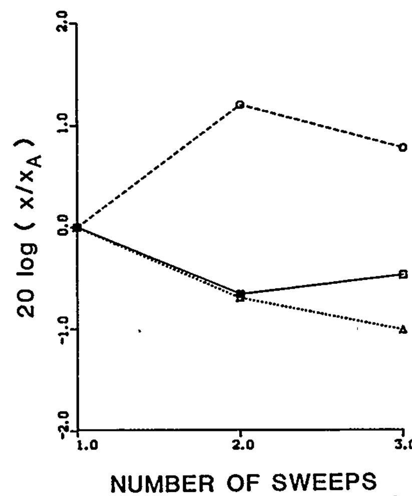

FIGURE 11d TOTAL SIDELOBE ENERGY

FIGURE 11 COMPARISON OF OBSERVATIONS FOR $\Phi_D = \delta, \Phi_M$ & Φ_{MP} ($N \leqslant 3$)

sidelobe energy is reduced as a result of the decrease in primary lobe energy (Fig. 11d).

Fig. 12 demonstrates the small change in primary lobe amplitude for a three-autocorrelation combination but the overall shape of ϕ_A has not been changed.

5.3.4 Observations for Different Constraints on Weighting Factors

When considering a linear combination of autocorrelation functions, Werner and Krey [70] did not consider weighting factors and essentially their method assumed $a_K = 1$ for all k. The formulation used in this thesis allowed the more general case $a_K \varepsilon \mathbb{R}$. However, the calculation of weights (see section 4.2.2) increases the computation time required to reach a solution to eqn. 4.4. Thus, it is important to examine whether calculating weights yields a more significant change in the shape of ϕ_A than assuming that $a_K = 1$.

Fig. 13 shows a comparison of observations for the two different constraints on the weighting factors. The minimum norm values (Fig. 13a) for $\phi_D = \phi_M$ and ϕ_{MP} demonstrate a more significant change in ϕ_A when $a_K \varepsilon \mathbb{R}$ than when $a_K = 1$. By examination of the change in

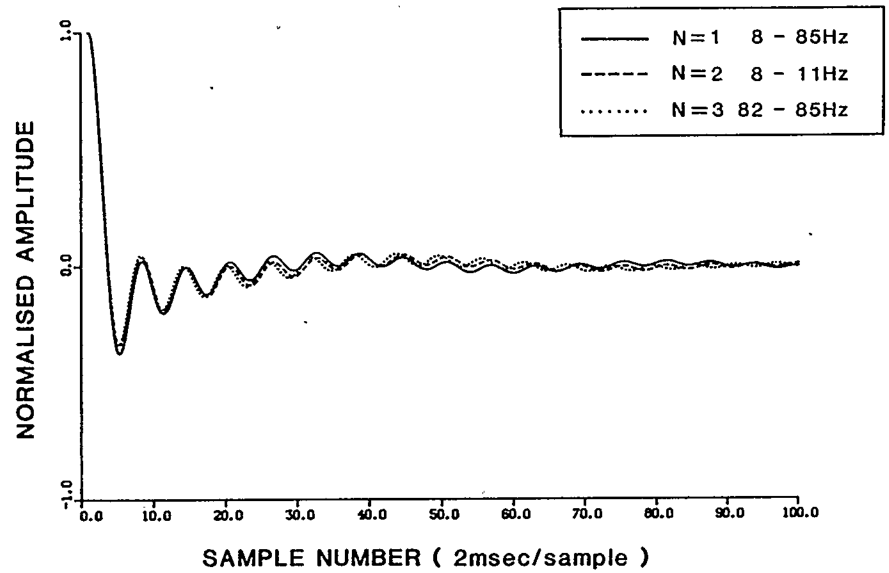

FIGURE 12 RESULTANT AUTOCORRELATION FUNCTION COMBINATIONS ($N \leq 3$) FOR $\Phi_D = \delta$

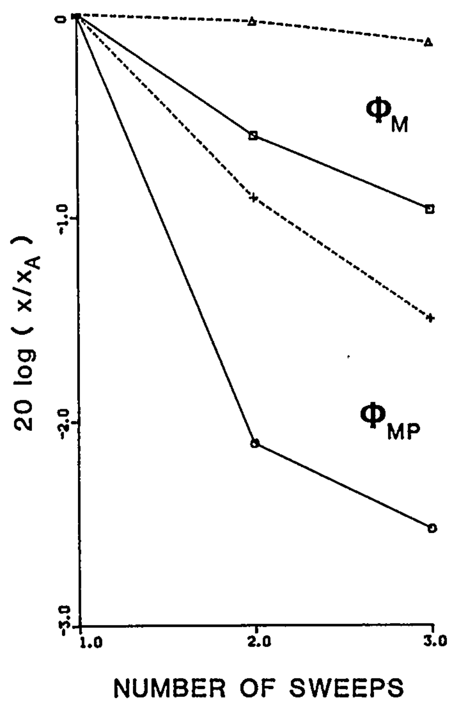

FIGURE 13 a MINIMUM NORM VALUES

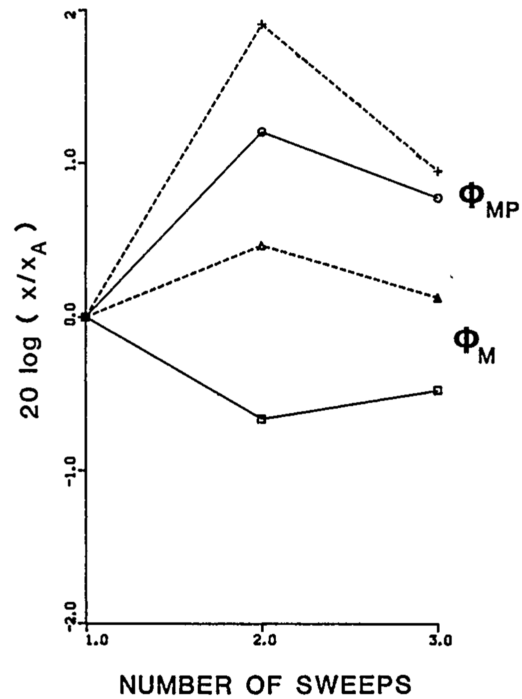

FIGURE 13 b TOTAL SIDELOBE ENERGY

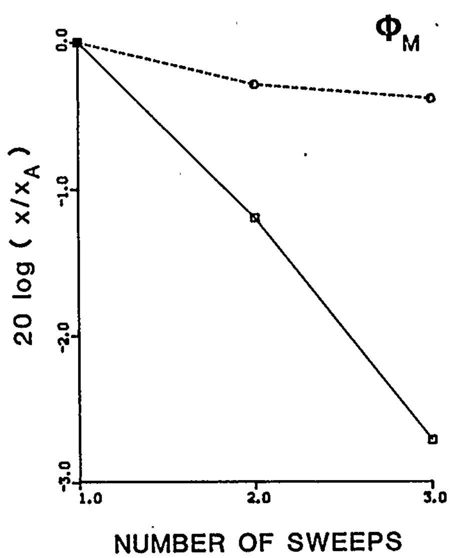

FIGURE 13 c A_p/A_m

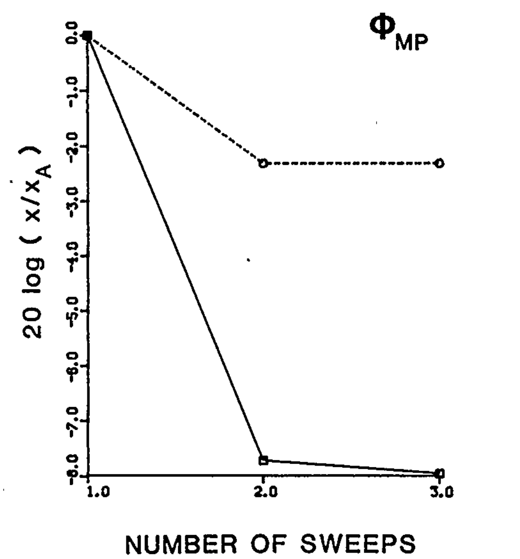

FIGURE 13 d FAR SIDELOBE ENERGY

FIGURE 13

COMPARISON OF OBSERVATIONS FOR

$a_k = 1$ AND $a_k \in \mathbb{R}$ FOR $\Phi_D = \Phi_M$ & Φ_{MP}

LEGEND

——— $a_k \in \mathbb{R}$

- - - - - - $a_k = 1$

total sidelobe energy, primary lobe amplitude and far sidelobe energy it is immediately apparent that, in all aspects, the constraint $a_K = 1$ inhibits the ability of the method to change the shape of ϕ_A more so than the more general constraint $a_K \in \mathbb{R}$.

5.3.5 Discussion

When $\phi_D = \phi_M$ the primary lobe energy is decreased and the far sidelobe energy is increased. Is the decrease in primary lobe energy greater than the increase in far sidelobe energy? It would at first seem that it would be easy to answer this question from the curve of the total sidelobe energy (Fig. 9). However, there is an increase in the main peak width that, because of the expression used to calculate sidelobe energy (eqn. 5.3), would show a decrease in sidelobe energy even for no change in the energy of the primary lobe and far sidelobes.

The apparent sudden decrease in total sidelobe energy (Fig. 8) is the result of an increase in main peak width of 1 sample i.e. 2 msec. If a smaller sample interval had been used then the decrease in total sidelobe energy would not have been so dramatic and would have decreased along a curve similar to the dashed line proposed in Fig. 8. This is supported by the increase in main peak width that is evident in Fig. 9 for $N \leqq 3$. However, because of the 2 msec sample interval that was used, Fig. 9 gives, for $N \leqq 5$, the total sidelobe energy assuming no increase in main peak width. This allows the conclusion that total sidelobe energy is reduced for $\phi_D = \phi_M$ and thus the decrease in primary lobe energy is greater than the increase in far sidelobe energy.

When $\phi_D = \phi_{MP}$ there is no change in the main peak width of ϕ_A and Fig. 9 shows an increase in total sidelobe energy. Thus the increase in the primary lobe energy, shown in Fig. 6, is greater than the significant reduction in far sidelobe energy. The behavior of the total sidelobe energy when $\phi_D = \delta$ was not examined because the changes in the shape of ϕ_A for $N \leqq 3$ were insignificant, as can be seen in Fig. 12.

Thus, as anticipated, ϕ_M is the only choice of ϕ_D for which there is a decrease in the total sidelobe energy. It is also the case for which the most significant change in ϕ_A occurred, namely the 30% decrease in the primary lobe amplitude. However, the decrease in total sidelcbe energy is accompanied by a small increase in the main peak width of ϕ_A. For $N \leqq 3$, the increase is only a small percentage of the main peak width and is tolerable.

The overall change in the shape of ϕ_A, regardless of the choice of ϕ_D, is not very significant as can be seen in Figs. 9, 10, and 12. The largest change occurred for $\phi_D = \phi_M$ when there was a 30% decrease in the primary lobe amplitude. This represents a significant change in one feature of the autocorrelation but it remains to be seen whether the changes in the shape of ϕ_A will be noticeable on field data (section 5.4).

The choice of ϕ_D determines the nature of the change in the shape of ϕ_A. If $\phi_D = \delta$ the method attempts to reduce the main peak width, primary lobe energy, and far sidelobe energy of ϕ_A. However, little change in the shape of ϕ_A occurs as can be deduced from the small change in the minimum norm values for each additional autocorrelation combined with ϕ_A, shown in Fig. 11. For $\phi_D = \phi_M$ the change in the minimum norm values is more significant than for $\phi_D = \delta$, and for $\phi_D = \phi_{MP}$ the change is even more significant (Figs. 5 & 11). This indicates that when ϕ_D is chosen such that the method is attempting to alter several features of ϕ_A the overall change in the shape of ϕ_A is smaller than if ϕ_D is chosen to alter fewer features e.g. reducing only far sidelobe energy.

The significant changes in the minimum norm values, regardless of the choice of ϕ_D, occur for $N \leqq 6$ (Fig. 5), with the norm values remaining relatively constant for

$7 \leqq N \leqq 20$. This implies the most significant changes in the shape of ϕ_A occur for $N \leqq 6$, with very little further change when more additional autocorrelations are considered. This is an important observation because it implies that when attempting to improve the shape of ϕ_A by combination with autocorrelation functions of linear sweeps, it is only necessary to consider a maximum number of six autocorrelations. For the thesis problem of reducing the total sidelobe energy of ϕ_A, which has been demonstrated to only occur when $\phi_D = \phi_M$, the significant change in minimum norm value occurs for $N \leqq 3$. Thus, if the method were to be applied in the field to reduce sidelobe energy, it would not be impractical to implement because only three different linear sweeps would have to be used.

5.3.6 Summary

The method succeeded in reducing the sidelobe energy of ϕ_A when $\phi_D = \phi_M$, a symmetrical function with the same main peak as ϕ_A and zero sidelobe energy. However, accompanying the reduction in sidelobe energy was a very small increase in the main peak width. The overall change in the shape of ϕ_A was not significant, although the primary lobe amplitude was decreased by as much as 30%, and it remains to be seen whether the changes will be noticeable in field data.

The ability of the method to change the shape of ϕ_A was found to be dependent on the choice of ϕ_D. If ϕ_D was chosen to induce changes in more than one feature of ϕ_A e.g. $\phi_D = \delta$ to attempt to decrease far sidelobe energy, primary lobe energy and main peak width, then the change in shape of ϕ_A was less than if ϕ_D was chosen to induce a change in only one feature of ϕ_A e.g. $\phi_D = \phi_{MP}$ to reduce only far sidelobe energy.

When attempting to reduce total sidelobe energy of ϕ_A the most significant changes in the shape of ϕ_A occur for $N \leqq 3$. This implies that the thesis method would not be impractical to apply in the field as only three different linear sweeps would have to be considered.

The constraint $a_K = 1$ for all values of k inhibits the ability of the method to change the shape of ϕ_A. In all aspects, allowing $a_K \in \mathbb{R}$ induced more significant changes in ϕ_A.

5.4 Field Test Results

5.4.1 Aim of the Field Test

The computer tests demonstrated that the total sidelobe energy of ϕ_A could be reduced by linear combination with other autocorrelation functions. However, of particular interest, is whether the resultant change in the shape of ϕ_A is sufficient to be noticeable on field data ?

In an attempt to answer this question, the three linear sweeps that formed the solution for $\phi_D = \phi_M$ for N = 3 were used in a field program. The aim of the field test was to examine whether the combination of the autocorrelation functions of the three linear sweeps would give data of higher quality than data generated by the largest bandwidth linear sweep.

5.4.2 Field Implementation

The linear sweeps that formed the solution of the thesis problem when $\phi_D = \phi_M$ and N = 3 were 8-11 Hz and 52 -83 Hz. The largest bandwidth sweep was 8-85 Hz. Each of the sweeps was of 6 seconds duration with a 250 msec cosine amplitude taper applied to each end (see section 5.2.1).

A standard field arrangement for the Vibroseis technique was used, with four vibrators shooting at 21 shot points, each 50 m apart, with 6 sweeps/vibrator/shot point. The station interval was 25 m. The line was shot three separate times, once for each sweep, with the data being recorded at 2 msec/sample.

After the data had been correlated, the different weights (a_1, a_2, a_3) were applied to the individual records, which were then stacked before any gain was applied. Both sections were processed in the same manner, using the same parameters so that any differences in the final sections would not be a result of differences in processing. The single-sweep section, for the largest bandwidth sweep, is shown in Fig. 14 and the three-sweep combination section is in Fig. 15.

5.4.3 Discussion

Examination of Figs. 14 and 15 show no visual difference in the section for the 8-85 Hz single linear sweep section and the section for the weighted combination of the 8-85 Hz, 8-11 Hz, 52-83 Hz linear sweeps. Thus the changes in the shape of the 8-85 Hz linear sweep autocorrelation (ϕ_A) that were demonstrated in the computer tests were not sufficient to give any noticeable improvement in the quality of field data.

The most likely reasons that the improvements in ϕ_A are not apparent are noise and the various filtering effects, represented by e(t) in eqn. 1.5, that were not accounted for in the development of the method. The improvements in the

SINGLE LINEAR SWEEP DATA (8 - 85Hz)

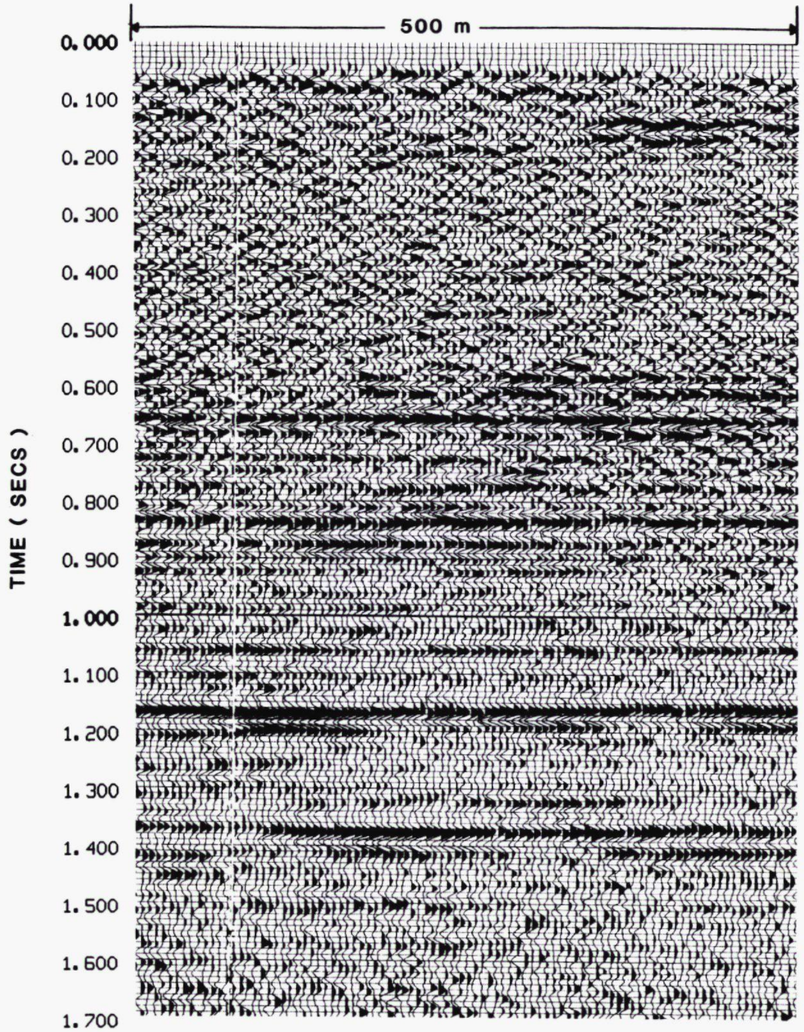

FIGURE 14

THREE SWEEP COMBINATION DATA
(8 - 85Hz, 8 - 11Hz, 52 - 83Hz)

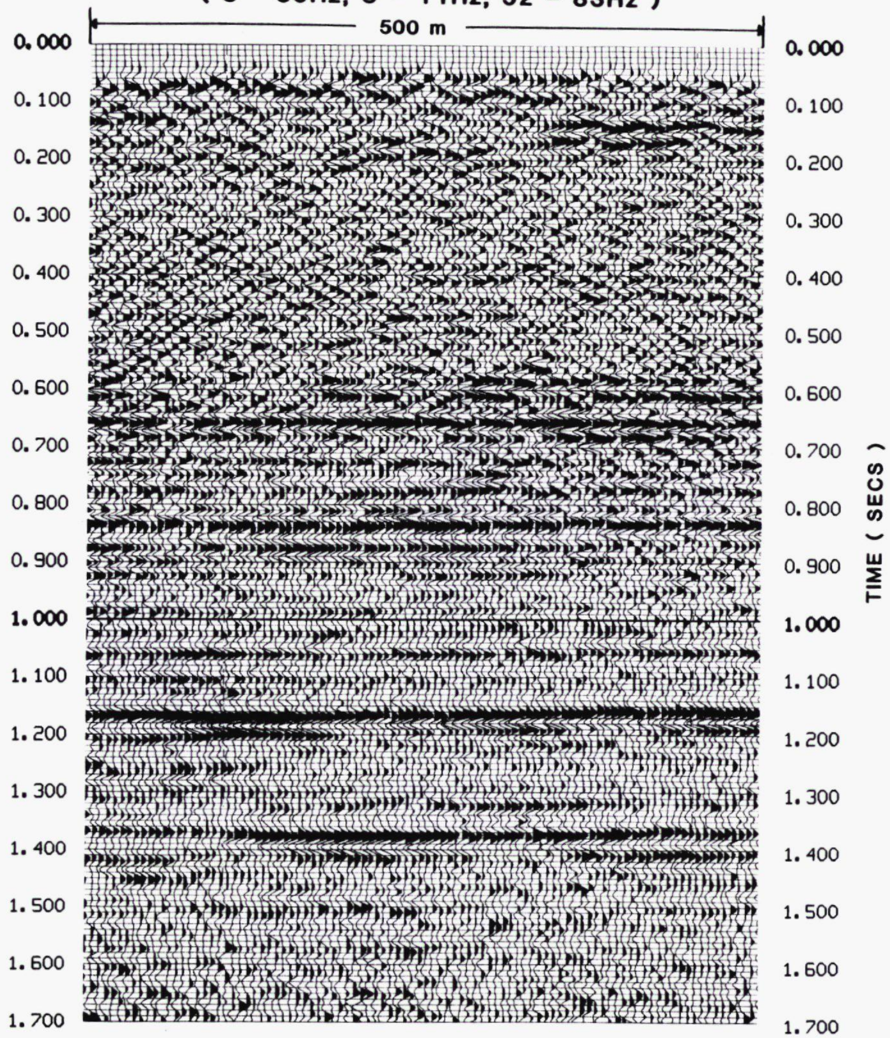

FIGURE 15

shape of ϕ_A were not significant enough to overcome the effects of noise and the various filters (see chapter I).

How can these effects be overcome ? If noise and the filter effects were to be accounted for in the method it would be necessary to find a set, or sets of nonlinear sweeps for which the method would select autocorrelation combinations that change the shape of ϕ_A significantly enough so that they are not overcome by the effects of noise and the various filters.

CHAPTER VI CONCLUSIONS

The computer tests discussed in chapter V show that, for linear sweeps in a particular bandwidth, the sidelobe energy of the autocorrelation function ϕ_A, of the largest bandwidth sweep, can be reduced by linear combination with other optimally selected autocorrelation functions. However, at best, the method only reduced the total sidelobe energy by 10%, the result of a 30% decrease in the primary lobe amplitude, but the main peak resolution was essentially preserved.

Field tests demonstrate that improvements in autocorrelation shape, that were seen in the computer tests, were not significant enough to yield an observable improvement in data quality. It is suggested that this is due to noise and various filtering effects, for example vibrator-earth coupling and frequency absorption, that overcome the improvements that were noticeable in the computer tests.

To account for noise and the filter effects, using the method described, it will be necessary to find a set, or sets, of nonlinear sweeps for which the reduction in sidelobe energy of a particular autocorrelation function would be significant enough not to be overcome by noise and the filter effects.

The algorithm described in the thesis has the advantage of generality, allowing for expansion to include different sweep definitions and constraints. The combinatorial search method that was used to solve for the frequency parameters had the major advantage of being stable. However, it involved large amounts of computation which restricted the size of the problem that could be solved.

In conclusion, the aim of the thesis, which was to minimize the sidelobe energy of a particular autocorrelation function using linear sweeps, was achieved. However, the reduction was not significant enough to improve the visual quality of field data. It is suggested that future work should consider the effects of noise and various filter effects, particularly vibrator-earth coupling and frequency absorption, by examining optimal combinations of the autocorrelation functions of suitably selected nonlinear sweeps.

BIBLIOGRAPHY

1. Alonso, M., and Finn, E.J., 1980, Fundemental University Physics, v.3, 11th edn., Addison-Wesley, London.

2. Anderson, J.A., 1969, Real Analysis, Gordon & Breach, New York.

3. Anstey, N.A., 1964, Correlation techniques - a review, Geophys. Prospect.,v.12, pp355 - 382.

4. Attewell, P.B., and Ramana, Y.V., 1966, Wave attenuation and internal friction as functions of frequency in rocks, Geophysics, v.31, pp1049 - 1056.

5. Berkhout, A.J., 1984, Seismic resolution, Handbook of Geophysical Exploration, Sec.1,v.12, Geophysical Press.

6. Bernault, T., and Peacock, J.H., 1978, Encoding techniques for the Vibroseis system, Geophys. Prospect., v.26, pp189-192.

7. Blum, E.K., 1972, Numerical analysis and computation: theory and practise, Addison-Wesely, London.

8. Bracewell, R.N., 1978, The Fourier transform and its applications, 2nd edn., McGraw-Hill, New York.

9. Brent, R.P., 1972, Algorithms for minimization without derivatives, Prentice-Hall, Englewood Cliffs, New Jersey.

10. Chaperson, A., and Labudene, B., 1983, Use of nonlinear sweeps for generation of high frequency data in Vibroseis, presented at the 53rd Annu. SEG Meet., Las Vegas, NV.

11. Chapman, W.L., Brown, G.L., Fair, D.W., 1981, The Vibroseis system: a high frequency tool, Geophysics, v.46, pp1657 - 1666.

12. Cook, C., and Bernfeld, M., 1967, Radar signals - an introduction to theory & practise, Academic Press, New York.

13. Crawford, J.M., Doty, W.E.N., and Lee, M.R., 1960, Continuous signal seismograph, Geophysics, v.25, pp95 - 105.

14. Cunningham, A.B., 1979, Some alternative vibrator signals, Geophysics, v.44, pp1901 - 1921.

15. Dobrin, M., 1976, Introduction to geophysical prospecting, 3rd edn, McGraw-Hill, New York.

16. Dolph, C., 1946, A current distribution for broadside arrays which optimizes the relationship between bandwidth and sidelobe level, Proc. IRE, v.34, pp335 - 348.

17. Edelmann, H.A.K., 1966, New filtering methods with Vibroseis, Geophys. Prospect., v.14, pp455 - 469.

18. ________________ , and Werner, H., 1982, The encoded sweep technique for Vibroseis, Geophysics, v.47, pp809-818.

19. ________________________________ , 1982, Combined sweep signals for correlation noise suppression, Geophys. Prospect., v.30, pp786 - 812.

20. Evans, R.J., Cantoni, A., and Anderson, B.D.O., 1980, Theoretical aspects of optimal autocorrelation synthesis, Information Sciences, v.22, pp171 - 199.

21. Fletcher, R.,1980, Practical methods of optimization, v.1, Wiley, New York.

22. _____________ , and Powell, M.J.D., 1963, A rapidly convergent descent method for minimization, Computer J., v.6, pp163 - 168.

23. _____________ , and Reeves, C.M., 1964, Function minimization by conjugate gradients, Computer J., v.7, pp149 - 154.

24. Forsythe, G.E., Malcolm, M.A., and Moler, C.B., 1977, Computer methods for mathematical computations, Prentice-Hall, Englewood Cliffs, New Jersey.

25. Friedman, F.L., and Koffman, E.B., 1981, Problem solving and structured programming in fortran, 2nd edn., Addison-Wesley, London.

26. Futterman, W., 1962, Dispersive body waves, J. Geophys. Research, v.67, pp 5279 - 5292.

27. Geyer, R.L., 1969, Vibroseis parameter optimization, Oil and Gas Journal, April 13 and April 27, 1970 editions.

28. ____________ , 1970, The Vibroseis system of seismic mapping, CSEG J., v.6, pp39 - 1304.

29. ____________, 1969, Catalog of Klauder wavelets, Tulsa, Seismograph Service Corp.

30. Goupillaud, P.L., 1976, Signal design in the Vibroseis technique, Geophysics, v.41, pp1291 - 1304.

31. Graybill, F.A., Meyer, C.D., and Painter, R.J., 1966, Note on the computation of the generalized inverse of a matrix, SIAM Rev., v.8, pp522 - 524.

32. Grenville, T.N.E., 1959, The pseudoinverse of a rectangular or singular matrix and its application to the solution of systems of linear equations, SIAM Rev., v.1, pp38 -43.

33. __________________, 1960, Some applications of the pseudoinverse of a matrix, SIAM Rev., v.2, pp15 - 22.

34. __________________, 1966, Note on the generalized inverse of a matrix product, SIAM Rev., v.8, pp518 - 521.

35. Gurbuz, B.M., 1972, Signal enhancement of vibratory source data in the presence of attenuation, Geophys. Prospect., v.20, pp421 - 438.

36. Hildebrand, F.B., 1974, Introduction to numerical analysis, 2nd edn., McGraw-Hill, New York.

37. Hoover, G.M., Gallagher, J.G., Rigdon, H.K., 1984, Vibrator signals, Proc. IEEE, v.72, pp1290 - 1301.

38. Kanasewich, E.R., 1981, Time sequence analysis in geophysics, 3rd edn., Univ. of Alberta Press, Edmonton.

39. Klauder, J.R., Prince, A.C., Darlington, S., and Albershiem, W.J., 1960, The theory and design of chirp radars, Bell Syst. Tech. J., v.39, pp745 - 808.

40. Krey, T., 1969, Remarks on the signal-to-noise ratio in the Vibroseis system, Geophys. Prospect., v.17, pp206 - 218.

41. Lancaster, P., 1969, Theory of Matrices, Academic Press, New York.

42. Landrum, R.A., 1967, Extraction of signals from random noise by cross correlation, presented at 37th Annu. SEG Meet., Oklahoma City, OK.

43. Lasdon, L.S., 1970, Optimization theory for large systems, McMillan, New York.

44. Lawson, C.L., and Hanson, R.J., 1974, Solving least squares problems, Prentice-Hall, New Jersey.

45. Lee, Y.W., 1960, Statistical theory of communication, Wiley, New York.

46. Lipschutz, S., and Poe, A., 1978, Programming with fortran, Schaum Outline Series, McGraw-Hill, New York.

47. Mack, H., 1966, Attenuation of controlled wave seismograph signals cbserved in cased boreholes, Geophysics, v.31, pp206 - 218.

48. Marquart, D.W., 1963, An algorithm for least squares estimation of nonlinear parameters, SIAM J., v.11, pp431-441.

49. McDonal, F.J., Angona, F.A., Mills, R.L., Sengbrush, R.L., Van Nostrand, R.G., and White, J.E., 1958, Attenuation of shear and compressional waves in Pierre Shale, Geophysics, v.23, pp421 - 439.

50. Nash, J.C., 1979, Compact numerical methods for computers: linear algebra and function minimization, Adam Hilger, Bristol, England.

51. O'Brien, P.N.S., 1961, A discussion on the nature and magnitude of elastic absorption in seismic prospecting, Geophys. Prospect., v.9, pp261 - 275.

52. Ortega, J.M., 1972, Numerical analysis, Academic Press, New York.

53. Parasnis, D.S., 1972, Principles of applied geophysics, 2nd edn., Chapman & Hall, London.

54. Penrose, R., 1955, A generalized inverse for matrices, Proc. Cambridge Philos. Soc., v.51, pp406 - 413.

55. Powell, M.J.D., 1964, An efficient method for finding the minimum of a function of several variables without calculating derivatives, Computer J., v.7, pp155 - 162.

56. _______________, 1966, Minimization of functions of several variables, In Numerical Analysis: an introduction, pp143 - 157, J. Walsh, ed., Academic Press, London.

57. _______________, 1970, A survey of numerical methods for unconstrained optimization, SIAM Rev., v.12, pp79 - 97.

58. Rietsch, E., 1977, Vibroseis signals with prescribed power spectrum, Geophys. Prospect., v.25, pp613 - 621.

59. ____________ , 1977, Computerized analysis of Vibroseis signal similarity, Geophys. Prospect., v.25, pp541 - 522.

60. Rihaczek, A., 1969, The principles of high resolution radar, McGraw-Hill, New York.

61. Robinson, E.A., 1967, Multichannel time series analysis with digital computer programs, Holden Day, San Francisco.

62. Seriff, A.J., and Kim, W.H., 1970, The effect of harmonic distortion in the use of vibratory surface sources, Geophysics, v.35, pp234 - 246.

63. Slepian, D., Landau, H., and Pollack, H., 1961, Prolate spheroidal wave functions, fourier analysis and uncertainty principle, Bell Syst. Tech. J., v.40, pp43 - 84.

64. Stewart, C.E., and Palace, J., 1983, eds. Numerical methods, software and analysis: IMSL Reference Edition, McGraw-Hill, New York.

65. Stewart, G.W., 1973, Introduction to matrix computations, Academic Press, New York.

66. Strang, G., 1980, Linear algebra and its applications, 2nd edn., Academic Press, New York.

67. Telford, W.M., Geldart, L.P., Sheriff, R.E., and Keys, D.A., 1976, Applied geophysics, Cambridge Univ. Press, Cambridge.

68. Traub, J.F., 1964, Iterative methods for the solution of equations, Prentice-Hall, Englewood Cliffs, New Jersey.

69. Vakman, D., 1968, Sophisticated signals and the uncertainty principle in radar, Springer, New York.

70. Werner, H., and Krey, Th., 1979, Combisweep - a contribution to sweep techniques, Geophys. Prospect., v.27, pp78 - 105.

71. Wuenschel, P.C., 1965, Dispersive body waves - an experimental study, Geophysics, v.30, pp539 - 551.

72. Vandergraft, J.S., 1983, Introduction to numerical computations, 2nd edn., Academic Press.

APPENDIX A

The Vibroseis Seismogram Trace

Using the convolution model [47] of the seismic trace, the signal recorded at the geophones is

$$g(t) = \{ s(t) * e(t() * r(t) \} + n(t) \qquad \text{A1}$$

where r(t) is the earth impulse response, n(t) is noise, s(t) is the seismic source signal, and e(t) represents the filtering effects of earth attenuation, vibrator plate - earth coupling and the recording system [9]. The correlation of the geophone output, g(t) and the vibrator input signal, s(t) yields the vibroseis seismogram trace

$$v(t) = s(t) \otimes g(t) \qquad \text{A2}$$

where $\otimes$ represents correlation. Substituting eqn. A1 into eqn. A2 gives

$$v(t) = s(t)\ X\ \{ [s(t) * e(t) * r(t)] + n(t) \}$$

$$= \{ s(-t) * s(t) * e(t) * r(t) \} + s(-t) * n(t) \qquad \text{A3}$$

The autocorrelation function of the signal s(t) is defined as

$$\phi_{ss}(t) = s(-t) * s(t) \qquad \text{A4}$$

and eqn A3 can be written

$$v(t) = \phi_{ss}(t) * e(t) * r(t) + N(t) \qquad \text{A5}$$

where $N(t) = s(-t) * n(t)$.

APPENDIX B

Calculation of The Number of Parameter Pairs Examined

There are two possible methods for implementing the combinatorial search method for solving for the frequency parameters in eqn. 4.4: considering only one additional autocorrelation at a time or considering all autocorrelation functions together. The total number of frequency parameters to be considered for each method (eqns. 4.5 and 4.6) are derived as follows.

Let there be P possible frequency parameter pairs allowed by the frequency constraint of eqn. 2.4. The frequency parameter pair for k = 1 is known. Also, it is assumed that a particular frequency parameter pair need only to be chosen once e.g. the case

$$a_1\phi_A + a_2\phi_2\ (\ f_2(0),\ f_2(T)\ ) + a_3\phi_3\ (\ f_3^{(R)}(0),\ f_3^{(R)}(T)\ )$$

where $f_2(0) = f_3^{(R)}(0)$ and $f_2(T) = f_3^{(R)}(T)$ does not need to be examined, since ϕ_2 and ϕ_3 are then the same autocorrelation function and if this combination was a solution to eqn. 4.4 (section 4.2), the weighting factor a_2 would have been calculated appropriately when k = 2.

B.1 Solving for One Autocorrelation Function at a Time

The parameter pair for k = 1 is known. Since the same pair cannot be chosen more than once, this leaves (P - 1) pairs to be considered for k = 2, which leaves (P - 2) pairs to be considered for k = 3. Similarly, for k = N, (P - (N - 1)) pairs are considered.

The total number of parameter pairs to be considered is then

$$(P - 1) + (P - 2) + \ldots + (P - (N - 1))$$

$$= P(N - 1) - (1 + 2 + 3 + \ldots + (N - 1))$$

$$= P(N - 1) - N(N - 1)/2 \qquad \text{B1}$$

B.2 Solving for All Autocorrelation Functions Simultaneously

Given that the frequency parameter pair for k = 1 is known, this leaves (P - 1) frequency parameter pairs from which (N -1) pairs have to be chosen. It is well known from elementary mathematics that the total number of combinations of n things taken r at a time is given by

$$\frac{n!}{r!\,(n-r)!}$$

Thus, the total number of (P - 1) things taken (N - 1) at a time is given by

$$\frac{(P-1)!}{((P-1)-(N-1))!\,(N-1)!}$$

$$= \frac{(P-1)!}{(P-N)!\,(N-1)!} \qquad \text{B2}$$